Uniaxial Hugoniostat: A method for atomistic simulations of shocked materials

J.-B. Maillet,[1] M. Mareschal,[1] L. Soulard,[2] R. Ravelo,[3] P. S. Lomdahl,[4] T. C. Germann,[4] and B. L. Holian[4]
[1]*CECAM, ENS-Lyon, 46 allée d'Italie, 69364 Lyon Cedex, France*
[2]*CEA, Département de Physique Théorique et Appliquée, Boîte Postale 12, 91680 Bruyères-le-Châtel, France*
[3]*Department of Physics, University of Texas, El Paso, Texas 79968-0515*
[4]*Los Alamos National Laboratory, Los Alamos, New Mexico 87545*
(Received 12 September 2000; published 27 December 2000)

An new equilibrium molecular-dynamics method (the uniaxial Hugoniostat) is proposed to study the energetics and deformation structures in shocked crystals. This method agrees well with nonequilibrium molecular-dynamics simulations used to study shock-wave propagation in solids and liquids.

DOI: 10.1103/PhysRevE.63.016121 PACS number(s): 64.10.+h, 02.70.Ns, 62.50.+p, 62.20.Fe

I. INTRODUCTION

Shock waves and their effects have been studied at the atomistic level by non-equilibrium molecular-dynamics (NEMD) simulations for over two decades [1]. More recently, large-scale NEMD shock-wave simulations have been performed, some of them including several millions of atoms [2]. These simulations generally include the whole process, from the creation of the shock wave, to its propagation in the material until it reaches a steady wave, and eventually its emergence at a free surface. In these computationally expensive simulations, a significant amount of time is spent in calculating the dynamics of the unshocked material in order to achieve the steady state.

Another recent NEMD method [3], known as the ''ramjet'' or the analytical moving window, focuses the simulation upon a region surrounding the wave front by moving the computational window at the same speed as the shock wave. Planes of unshocked crystalline material are introduced on one side while slices of shocked material disappear on the other side. This method has been found to provide accurate information on the shock front structure, especially as obtained from profiles of the thermodynamic quantities versus distance from the front. If the profiles are steady in the region between the shock front and the window boundary, they can provide reliable values of shocked material properties, provided the processes involved in the relaxation of the material are short on the computational time and distance scales.

We propose in this paper an equilibrium molecular-dynamics (MD) technique for extracting both thermodynamic and structural properties of shocked crystalline solids and fluid, based on the Hugoniot relations for planar, steady shock waves and their inherently anisotropic nature. The thermodynamic quantities of a material in the initial unshocked state and the final shocked state are linked by the so-called Hugoniot conservation relations of mass, momentum, and energy across the shock front:

$$\text{mass:}\quad \rho_0 u_s = \rho(u_s - u_p)$$

$$\Rightarrow \epsilon = 1 - \rho_0/\rho = 1 - V/V_0 = u_p/u_s, \tag{1}$$

$$\text{momentum:}\quad P_{zz} = P_0 + \rho_0 u_s u_p$$

$$\Rightarrow u_s = \sqrt{\frac{P_{zz} - P_0}{\rho_0 \epsilon}},$$

$$u_p = \epsilon u_s, \tag{2}$$

$$\text{energy:} E = E_0 + \frac{1}{2}(P_{zz} + P_0)(V_0 - V). \tag{3}$$

E is the internal energy per unit mass, P_{zz} is the normal component of the pressure tensor in the direction of the shockwave (arbitrarily chosen to be the z-direction), and $V = 1/\rho$ is the volume per unit mass of the shocked material; subscript ''0'' refers to these quantities in the initial unshocked state. u_s is the shock velocity in the material produced by a piston moving into it at velocity u_p. ϵ is the compressive volumetric strain (compression).

These relations are often referred to as ''jump conditions'' since the initial values ''jump'' to the final values as the shock wave passes through the material. (Of course, the ''jump'' at the steady shock front is not instantaneous, but instead, takes place over a finite rise-time or spatial shock thickness. In this paper, we are interested in the *final state* long after the shock wave has passed through the material, and not in the actual simulation of the very interesting, but transient processes in the shock front.) The final states obtained for different shock strengths form the Hugoniot curve, which can be plotted either as a nearly straight line of u_s versus u_p, or as a nonlinear curve of P_{zz} versus V. [From the final long-time average of P_{zz}, u_s and u_p can be computed from Eqs. (1) and (2).]

We make a special point here of emphasizing the inherently anisotropic nature of the shock wave. Anisotropy is particularly important for solids, which can sustain nonzero shear stress and also defect structures, making their behavior quite distinct from that of fluids. While we are most interested in the final shocked states, we note that at the shock front, even in the case of fluids, the normal pressure P_{zz} is typically greater than the transverse components P_{xx} and P_{yy}, so that even fluids show transient anisotropic behavior. For later reference, the hydrostatic pressure is one-third the trace of the pressure tensor, $P = (P_{xx} + P_{yy} + P_{zz})/3$, and we

define the shear stress in planar shock wave geometry to be half the normal stress difference:

$$2\tau = P_{zz} - \tfrac{1}{2}(P_{xx} + P_{yy}), \tag{4}$$

so that we can write the normal pressure as

$$P_{zz} = P + \tfrac{4}{3}\tau. \tag{5}$$

In the case of fluids, the shear stress at the shock front is relieved by viscous flow in the transverse directions, so that the final state far behind the shock front is at hydrostatic equilibrium: $P_{zz} = P$ (or $\tau = 0$). In the case of solids, however, transverse motion can occur only if there is sufficient shear stress to overcome the inherent energy barrier to produce defects (e.g., dislocations) or else phase transformations, and thereby, plastic flow (deformation). In any case—whether or not there is plastic deformation—the final state in a solid is *still* not guaranteed to be hydrostatic, so that there can, in principle, be a residual (nonzero) shear stress.

Without simulating a shock wave, the states on the Hugoniot curve can be found by using the Hugoniot relations as constraints. By assumption, only the *final state* is important: its volume can be fixed at time zero by allowing atoms to vibrate around perfect, unstrained lattice sites (at volume V_0 and temperature T_0 in the cold, unshocked solid), and then applying homogeneous compression ϵ, which can be either uniaxial (in the *z*-direction only, as in the shock wave) or isotropic (in all three spatial directions). The final Hugoniot temperature can be reached by an equilibrium MD method, using a feedback thermostat to constrain the internal energy, according to the Hugoniot relation given by Eq. (3). We call this combination of initial compression and subsequent thermostatting ''the Hugoniostat.''

We expect that the choice for Hugoniostat initial conditions—either uniaxial or isotropic compression—will give rise to different results *only* in the case of a solid, but not for a fluid. Under isotropic strain in the solid, the time average of the normal pressures are all expected to be equal (so that $\tau = 0$), and we can therefore suppose that an isotropic initial condition will not relax, so as to produce any resulting defect structures, while the uniaxial initial condition will. In fact, we expect that the uniaxial Hugoniostat will produce plastic deformation more closely resembling a shock wave, by virtue of the anisotropy inherent in both of these compressive processes. The system sizes required for these two ''flavors'' of Hugoniostat will therefore also be quite different: in order for the uniaxial method to give a faithful rendering of the shockwave defect structures, the computational box will have to be big enough to contain a reasonable sample of the deformation, which will not in general be uniform in distribution. Moreover, depending on the natural relaxation time for the flow processes, it may still not be possible to observe the deformation on reasonable computational time scales. The model and the new equations of motion for the atoms are described below, followed by a study comparing direct NEMD shockwave and Hugoniostat equilibrium MD results.

II. THEORY

We propose new equations of motion, which constrain the system internal energy to lie on the shock Hugoniot curve (hence, we call this the ''Hugoniostat''). The shock strength is determined by the compressive volumetric strain, or compression ϵ. At time zero, we take a configuration of N atoms vibrating about unstrained crystal lattice sites (at volume V_0 and low temperature T_0), and then apply an instantaneous, homogeneous compression, either uniaxially or isotropically, bringing the system to a highly strained state at the final volume V.

The dynamical evolution of the system, in either of the compressional ''flavors'' of the Hugoniostat (either uniaxial or isotropic), is achieved by integral feedback that controls the internal energy, analogous to the method of thermostatting initially proposed by Nosé and modified by Hoover [4]. In our approach, in addition to the $3N$ particle coordinates $\mathbf{r}_i$ and momenta $\mathbf{p}_i$, we introduce a single intensive global degree of freedom—the heat-flow rate χ (negative into, or positive out of the system)—whose equation of motion depends on the instantaneous values of E and P_{zz}:

$$\dot{\mathbf{r}}_i = \frac{\mathbf{p}_i}{m}, \tag{6}$$

$$\dot{\mathbf{p}}_i = \mathbf{F}_i - \chi \mathbf{p}_i, \tag{7}$$

$$\dot{\chi} = \nu^2 \frac{E - E_0 - \frac{1}{2}(P_{zz} + P_0)(V_0 - V)}{N\epsilon_0}. \tag{8}$$

Equation (8) above assumes that the final state is in the uniaxially compressed solid phase. [Obviously, for isotropic compression of the solid or for a fluid, one is free to replace P_{zz} by P in this equation, just as in the Hugoniot expression Eq. (3).] The frequency ν is associated with the heat-flow rate χ: it is an input parameter chosen to optimize the efficiency of the coupling between the Hugoniostat and the system of atoms. (ϵ_0 is the unit of energy for the interaction potential and should not be confused with the symbol for compression.)

The feedback provided by the heat-flow rate χ guarantees that, at long times, the system reaches a temperature appropriate to the shocked state on the Hugoniot. This ''Hugoniostat'' provides a new statistical ensemble where the Hugoniot relation is satisfied in the long-time average. We emphasize that, like laboratory shockwave experiments, the Hugoniostat simulation gives the velocities u_s and u_p. But, in addition, the Hugoniostat calculation readily yields the shock temperature, which is not easy to measure in experiments.

III. METHODOLOGY

Results in this paper are presented for atoms interacting by the well-known Lennard-Jones 6-12 pair potential, using reduced units of distance to the minimum r_0, bond energy ϵ_0, atomic mass m, and time $\tau = r_0\sqrt{m/\epsilon_0}$; the potential is set to zero for distances beyond $2.23r_0$. We have performed

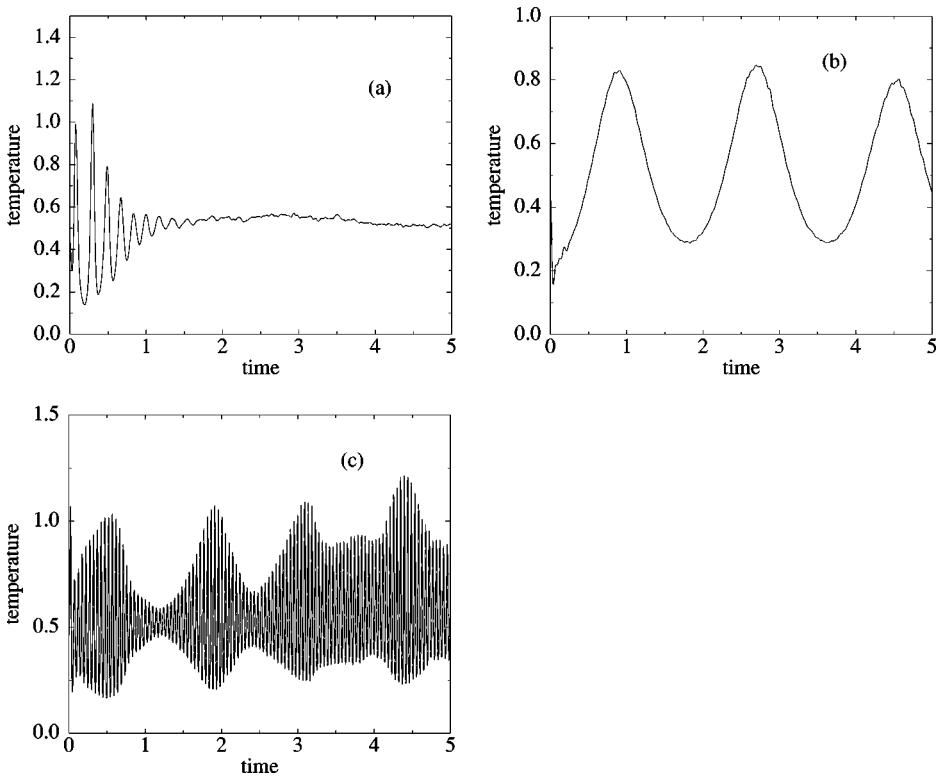

FIG. 1. (a) Time evolution of the temperature under uniaxial Hugoniostat (20% strain), with optimal coupling $\nu=33$; (b) with weak coupling $\nu=3.3$; (c) with strong coupling $\nu=100$.

simulations to compute the Hugoniot curve in three different ways, using the same initial equilibrated configuration, namely, an unstrained, zero-pressure, nearly zero-temperature ($kT_0/\epsilon_0=0.001$), face-centered cubic (fcc) crystal (the potential cutoff is just before the 5th neighbor shell).

First, we performed direct NEMD shockwave simulations in the solid, with the shockwave propagation along the $\langle 001\rangle$ crystal direction (i.e., along the z-axis) for typical sample sizes $30\times30\times150$ unit cells. To initiate the shock wave, the sample is given an average initial z-velocity of $-u_p$ and thrown into a momentum mirror standing at $z=0$ [2]. Periodic boundary conditions are applied in the x- and y-directions. One end of the sample is a free interface, while the other is confined by the momentum mirror. The simulation is run until the shock wave reaches the free end of the sample (a time of usually less than $10t_0$). Classical Newtonian equations of motion are integrated by central differences, with the timestep ranging from 10^{-3} to $2\times10^{-3}t_0$.

Next, in order to compare with the final states produced by these NEMD shockwave simulations, we performed equilibrium Hugoniostat MD simulations, both isotropic and uniaxial. In each case, the simulation box is originally a cube of size $15\times15\times15$ unit cells, with periodic boundary conditions applied in all three directions. An instantaneous compression is performed homogeneously, either isotropically or uniaxially along the $\langle 001\rangle$ (z-direction) at time $t=0$. The dynamic evolution of the system is then computed according to the equations of motion described in the previous section, typically for times of about $50t_0$. (Note that an MD Hugoniostat calculation is about 8 times less expensive than an NEMD shockwave.)

In the Hugoniostat MD simulations, the response time of the system is dictated by ν, the frequency (coupling strength) of the thermostat. In order to get an efficient coupling between the Hugoniostat and the system, ν should be chosen to be close to the natural vibrational frequency of the atoms, represented by the Einstein frequency ω_E under compression [5,6]. As the compression goes up, so does ω_E, and so should ν. To illustrate this, we show in Fig. 1 the difference in evolution of the temperature under three coupling strengths. When the coupling is chosen to mirror ω_E at 20% compression (about twice the value at normal density), the temperature comes quickly to its equilibrium value with modest, random-looking fluctuations. A value of ν that is too small gives rise to large, long-lived undulations in the temperature, while a value of ν that is too large exhibits large-amplitude oscillations that never seem to settle down.

Care has to be taken also with the initial value of the temperature. When a large strain (either uniaxial or isotropic) is applied to the system, the initial state can be quite far from the final equilibrium state, and the early stages of the simulation can exhibit very large fluctuations in the various mechanical quantities before settling down. In order to prevent unwanted instabilities, the temperature of the system is given an initial value obtained from the Hugoniot energy relation [Eq. (3)], where the potential part of the pressure P_{zz}^{Φ} and the potential energy Φ per unit mass are evaluated at the compressed volume V:

$$kT_{(t=0)}/m=2\frac{E_0+\frac{1}{2}P_{zz}^{\Phi}(V_0-V)-\Phi}{4-V_0/V}. \tag{9}$$

When the initial temperature is set according to Eq. (9), fluctuations larger in amplitude than those expected at equi-

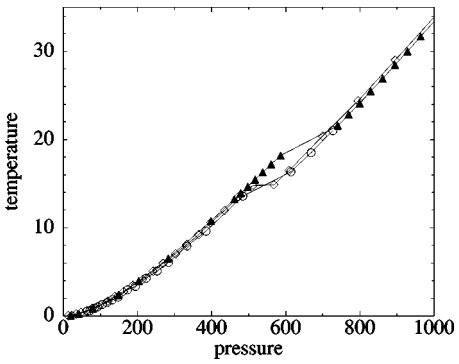

FIG. 2. Pressures and temperatures from simulations: NEMD shockwave (diamonds), uniaxial Hugoniostat (circles), and isotropic Hugoniostat (triangles).

librium are still observed in the early stages of the simulation, but they are considerably smaller than when the initial temperature is chosen to be too small. The initial values of χ and $\dot{\chi}$ are set to zero.

IV. RESULTS

A. Comparison of thermodynamic properties: NEMD and Hugoniostat

Using the direct NEMD method, shockwave simulations for different piston velocities have been performed, from small shock strength up to the melting transition. When the shock wave reaches the end of the sample, the thermodynamic quantities for the shocked material are averaged in space, excluding a few layers next to the shock front and next to the momentum mirror. In the case of the uniaxial and isotropic Hugoniostats, simulations at a variety of compressions have been performed. Averaging is done when the system has reached a stable state (namely, when the thermodynamic quantities fluctuate around a constant average value). Figure 2 shows pressures and temperatures along the Hugoniot, calculated using the three methods.

In the two Hugoniostat methods, the Hugoniot relation is guaranteed. In general, as we show in the following section, the uniaxial Hugoniostat produces defect structures very similar to the direct NEMD shockwave simulations, while no defects at all appear in the isotropic Hugoniostat simulations until well after melting has occurred along the shock Hugoniot. The good agreement found between the different Hugoniot curves then demonstrates that the thermodynamic quantities are insensitive to the presence of solid-state defects.

The Hugoniot relation is obeyed in the NEMD shockwave simulation provided the shock wave has traveled far enough to become steady. We note that for the strongest shocks—i.e., those that result in melting—the NEMD simulations have to be run for very long times to ensure steady-wave convergence to the fully melted state. In this regime, both the uniaxial and isotropic Hugoniostat simulations agree well with each other, and give more reliable results for much smaller system sizes than do the NEMD simulations.

The change seen around a pressure $P \approx 580$ is associated with the melting of the material. The uniaxial Hugoniostat MD and NEMD shockwave simulations agree very closely with each other, while the isotropic Hugoniostat differs noticeably near the melting point. The melting temperature obtained from the isotropic Hugoniostat is indeed found to be greater than the other two, suggesting that the solid is superheated under isotropic compression. When a crystal is isotropically compressed, defects are not produced in the structure, so that a significant mechanism for bulk melting in shock waves is suppressed. The crystal remains perfect up to the melting temperature.

Figure 3 shows a snapshot of the isotropic Hugoniostat simulation, just below melting, along with the radial distribution function (RDF). Since the temperature is very high, the RDF exhibits broad peaks, so that the perfect fcc character is not at all obvious in the snapshot. Nevertheless, pure fcc crystal is found after annealing this configuration. (The quench is done by kinetic annealing, where the velocities of all particles are set to zero whenever the total kinetic energy of the sample has passed through a maximum [7].)

B. Comparison of structural properties: NEMD and uniaxial Hugoniostat

Isotropic compression of a perfect fcc crystal does not generate any shear stress whatsoever, and shear stress is necessary to produce extended defects in the solid, such as pairs of partial dislocations. Thus, an isotropically compressed crystal remains completely free of extended defects until it melts. (Under periodic boundary conditions—especially for small system sizes—melting occurs in MD simulations at a noticeably higher temperature than the value at the thermodynamic limit.) On the other hand, a shock wave induces a

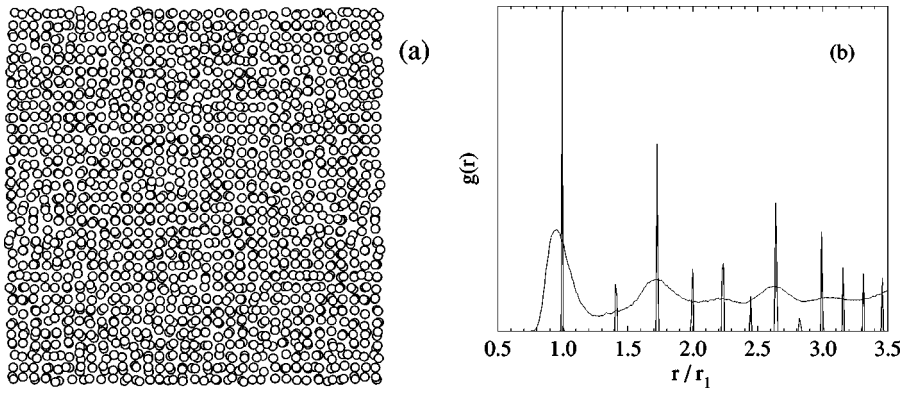

FIG. 3. (a) Snapshot of an (x,y) slice of the system at the end of an isotropic Hugoniostat simulation (36% strain). (b) RDF, compared with that of a zero-temperature fcc crystal. Radii for this RDF have been normalized to the nearest neighbor distance r_1.

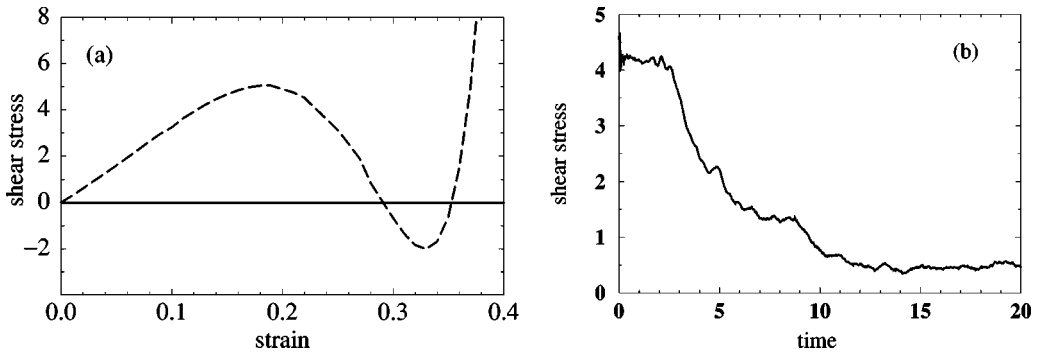

FIG. 4. (a) Initial shear stress for fcc ⟨100⟩ uniaxial compression at $T=0$, as a function of volumetric compression. (b) Time evolution of the shear stress in a uniaxial Hugoniostat simulation at 16% compression.

maximum value of the shear stress at the shock front, which is subsequently reduced as defects are created.

In comparing NEMD shockwave simulations with the equilibrium, homogeneous Hugoniostat methods, it is important to remember that shock waves are spatially inhomogeneous, with a finite thickness. There may be many important features, associated both with the gradient across the front and the transient time-dependence of the wave, that are not fully captured by the uniaxial Hugoniostat (even though it is anisotropic, like the shock wave). One important feature common to both—at least to some degree—is the anisotropy of the momentum distribution at the shock front, which could lead to thermal activation of defect creation.

In Fig. 4(a), we display the initial value of the shear stress $\tau(t=0)$ in the uniaxial Hugoniostat as a function of uniaxial compression ϵ along the ⟨100⟩ direction and at an initial temperature $T_0=0$. Note that there is a special symmetry point at $\epsilon=1-1/\sqrt{2}=0.293$, where the initial fcc lattice has been turned into bcc [8].

It has been found that, for fcc ⟨100⟩ shocks above a critical shock strength (near 14% strain), the shear stress is relieved by the emission of partial dislocations and the resulting formation of stacking faults on the four available {111} slip systems [2]. Similarly, shear stress is produced during ⟨100⟩ uniaxial compression of an fcc crystal. For strains up to 14%, the final structure is elastic uniaxially strained fcc, i.e., body-centered tetragonal (bct), and no defects are nucleated. However, at strains above 14%, the shear stress is relieved by the formation of defects in both the uniaxial Hugoniostat and NEMD simulations. At these strains, corresponding to moderate shock strengths, shear stress appears to be the driving force for the creation of extended defects. The relief of the shear stress can be seen in Fig. 4(b) which shows τ vs. time in an actual uniaxial Hugoniostat calculation at 16% compression. The shear stress drops to a lower value, after defects are produced. This mirrors the behavior in full NEMD shockwave simulations. As we shall see, deformation continues to occur well beyond the peak in the initial shear-stress curve. Consequently, initial shear stress is not a completely reliable diagnostic for predicting shock-induced plasticity; the processes are evidently more complicated.

Figure 5 displays a snapshot at the end of the uniaxial Hugoniostat simulation at 19% strain and also at the end of a shockwave simulation at the same strain ($u_p=2.5$). The snapshots of the plastic deformation resulting from the shock wave and uniaxial Hugoniostat look similar, indicating the presence of stacking faults in the crystal under both anisotropic processes. The size of the Hugoniostat sample is too small to get an accurate value of the density of defects produced. Nevertheless, the distance between two stacking faults seems to be approximately the same in both cases (the snapshots in Fig. 5 are for the same cross-sectional area). Analysis of the RDF for these two configurations confirms the nearly isotropic fcc character of the structure. Nevertheless, if these systems are kinetically annealed, very small bumps at $r=1.62$ and $r=1.89$ can be seen in the normalized RDF, representative of distances in the hexagonal close-packed (hcp) crystal, which is characteristic of fcc stacking faults (stacking of close-packed {111} planes goes from ABCABC... to ABABC...). It takes a time of approximately $10t_0$ for τ to be partially relieved via the creation of faults in the uniaxial Hugoniostat simulation. At the end of the simulation, τ is not zero. The value of the ''residual'' shear stress is mildly dependent on system size.

For higher compressions, in the range 15–23 %, stacking faults are the principal defects created, and their density increases with compression. This same trend is also observed in shockwave simulations and the density of stacking faults can be used as a measure of the plastic work [2].

At even greater compressions (or higher piston velocities), new deformation patterns are seen. Figure 6 displays a snapshot of a uniaxial Hugoniostat simulation at 26% com-

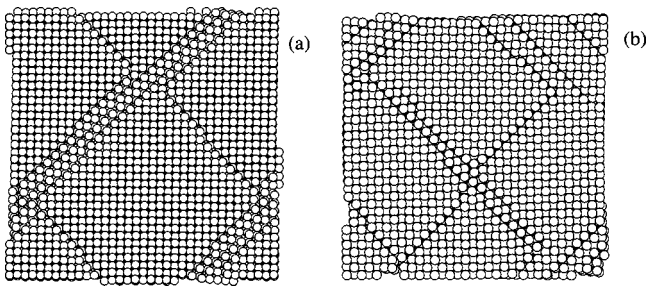

FIG. 5. (a) Snapshot of an (x,y) slice of the system at the end of a uniaxial Hugoniostat simulation (19% compression), after kinetic annealing. (b) Snapshot after a shock wave initiated with $u_p=2.5$ (18.5% compression) has propagated through the sample.

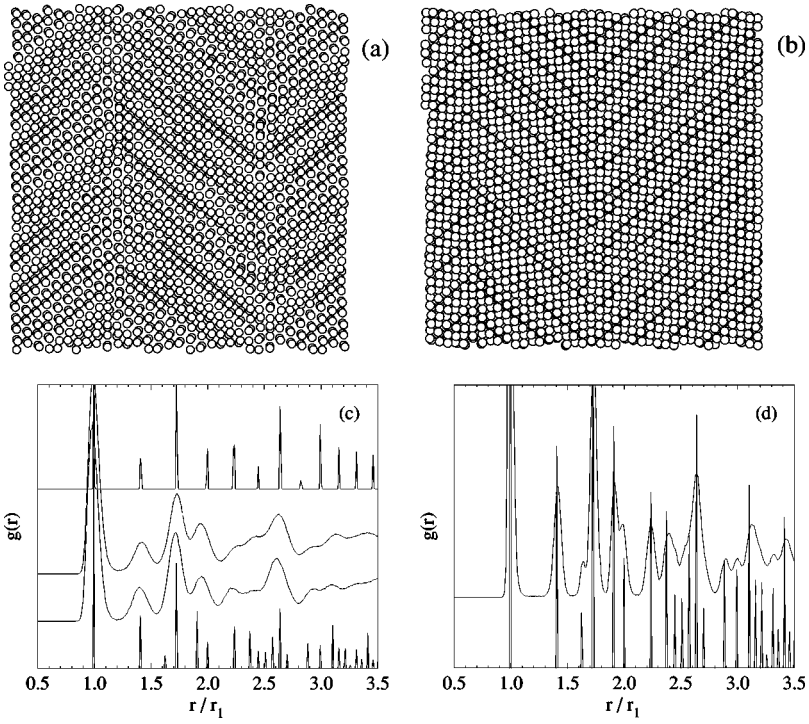

FIG. 6. (a) Snapshot of an (x,y) slice at the end of a uniaxial Hugoniostat simulation (26% compression), after kinetic annealing. (b) Snapshot after a shock wave ($u_p = 4.5$) has propagated into the sample. (c) RDFs from top to bottom: perfect (zero-temperature) fcc crystal, after passage of a shock wave (25.7% compression), after uniaxial Hugoniostat simulation (26% compression), and perfect hcp crystal. Radii for these RDFs have been normalized to r_1. (d) RDF of a perfect hcp crystal and selected chevron bands (see text) from a shockwave simulation (25.7% compression), after kinetic annealing.

pression, along with a snapshot of a shockwave simulation ($u_p = 4.5$, or 25.7% compression). The snapshots show the presence of similar defects as seen at lower strains, namely stacking faults, but the overall pattern is different from the ones seen at weak shock strength. We can see the appearance of ''chevron bands'' in the y-direction, where the system seems to have slipped along only one direction [for example, Fig. 6(a) exhibits two chevron bands of defects]. These bands appear sometimes in the x-direction (x- and y-directions are obviously equivalent at the beginning of the simulation). We notice that the distance between two bands seems to be approximately the same for the shockwave and uniaxial Hugoniostat simulations. The RDFs exhibit thermally broadened peaks, and comparison with the RDF of perfect hcp or fcc crystals is inconclusive. Kinetic annealing has been performed on the two systems in order to rapidly quench out thermal fluctuations, without changing the structure. One of the chevron bands has been extracted from the structure, and the corresponding RDF is displayed in Fig. 6(d), along with that of a perfect hcp crystal. The agreement

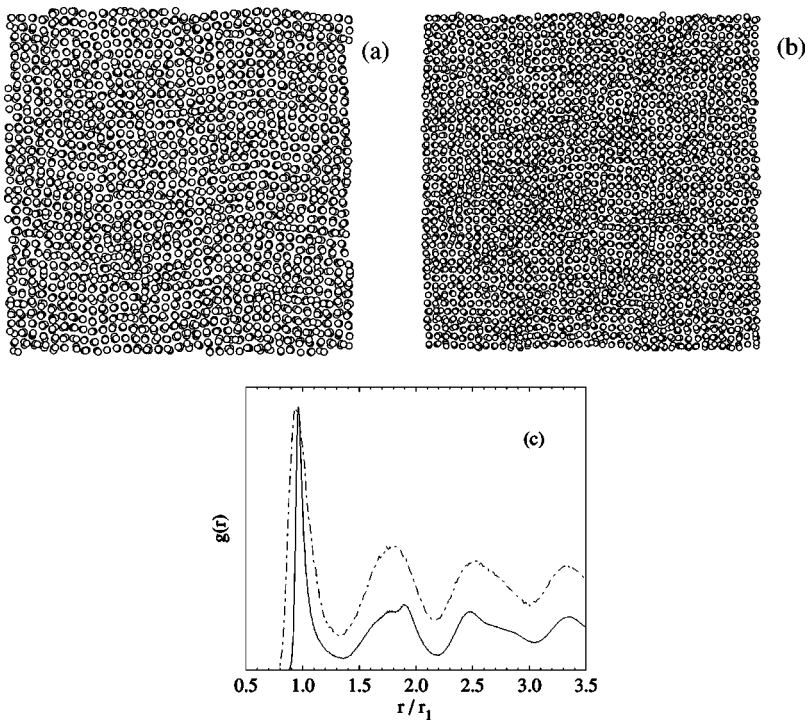

FIG. 7. (a) Snapshot at the end of a uniaxial Hugoniostat simulation (35% compression). (b) Snapshot at the end of a shockwave simulation ($u_p = 10.5$). (c) RDFs for the two simulations: uniaxial Hugoniostat (dot-dashed line) and shock wave (solid line).

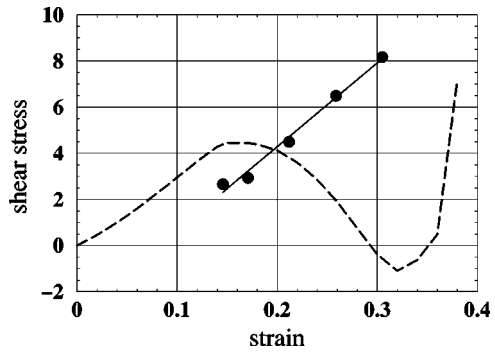

FIG. 8. Shear stress as a function of compression in the fcc ⟨100⟩ direction for the short-ranged Lennard-Jones potential ($r_{max} = 1.547 r_0$ [2]). The dashed curve is the *initial*, $T=0$ value in the uniaxial Hugoniostat; the solid circles represent the maximum shear stress at the shock front in direct NEMD shockwave simulations.

between the two is good, and no additional peaks are found. The resulting hcp structure contains a very high density of defects.

These chevron patterns in the hcp structure, characteristic of twins, are also observed for compressions in the range of 24–33 % for both shockwave and uniaxial Hugoniostat simulations. Shock-induced melting occurs around 36% compression. For compressions between 34% and 36%, new structures emerge, a snapshot of which can be seen in Fig. 7. The system is still ordered, but does not exhibit the same type of chevron patterns as previously described.

The structure of the system, and particularly the presence of defects, is essential to predict the correct melting behavior of a material under shock compression. In this regard, the uniaxial Hugoniostat is much more faithful to the direct NEMD shockwave simulation, compared to the isotropic Hugoniostat. When compared with direct NEMD simulations, the uniaxial Hugoniostat is able to not only reproduce the critical uniaxial strain above which plastic deformation is observed, but also the same structures and density of defects seen in direct shock simulations over a wide range of strains, all the way up to melting.

The similarities between the type of structures obtained in NEMD shock simulations and the uniaxial Hugoniostat notwithstanding, there remain important differences between the two approaches. In Fig. 8, we show the initial shear stress $\tau(t=0)$ for the uniaxial Hugoniostat ($T_0=0$, short-ranged Lennard-Jones potential [2]) as a function of compression. Also shown is the maximum shear stress at the middle of the NEMD shock wave. From this figure, we see that the initial shear stress above about 16% reaches a maximum and then falls. If this initial shear stress were all that were important to defect production in the perfect ⟨100⟩ fcc crystal, one might conclude that no plastic deformation ought to occur for shock waves whose strength is sufficient to produce compression above this peak value. Moreover, at the strain where $\tau(t=0)=0$, one could argue that no deformation of any kind should occur. It is clear from this figure that the maximum shear stress at the shock front is more predictive of the plastic deformation seen in fcc ⟨100⟩ shocks, particularly for compressions above the perfect-crystal threshold near 14%. There, the temperatures climb very nonlinearly with strain, so that thermal fluctuations—particularly significant for the overshoot seen in uniaxial shock waves, and mirrored notably in the uniaxial Hugoniostat simulations—cannot be ignored. Moreover, the structures seen in shock waves and in the uniaxial Hugoniostat at high compression depend upon details in the interatomic interaction potential. Belak [10] has noted a region of compression just before melting that appears to have no deformation, at least for one kind of interaction potential. Crystal stability and thermal activation of defect production—both dependent upon interaction potential—are just two factors that need to be considered in this region of high shock compression prior to melting.

V. CONCLUSIONS

A new equilibrium MD method—the uniaxial Hugoniostat—for simulating the final state of shocked crystals has been developed and successfully applied to the case of the Lennard-Jones fcc ⟨001⟩ crystal. This method homogeneously and uniaxially compresses the crystal instantaneously at time zero to the final shocked volume, and then couples the system to a thermostat that guarantees that the final Hugoniot state is achieved. Not only has the Hugoniot curve been successfully reproduced using this method, but also the defect structures produced by the shock wave. It has been shown that the deformation structure of the solid plays a key role in the determination of the correct melting point along the shock Hugoniot. In contrast, the use of isotropic compression does not produce defective structures until after the solid melts. On the other hand, uniaxial compression produces the same types of defects as the shock wave, all the way up to the melting transition. Thus, the uniaxial Hugoniostat is much better able to reproduce the energetics and structure of full NEMD shockwave simulations (provided, of course, that the computational volume is large enough to contain a representative portion of the defects). In any event, the uniaxial Hugoniostat is nearly an order of magnitude less expensive than a full shockwave simulation and has shown to be quite useful in the study of the wide range of structural changes seen as a function of compression. At low compression (up to 14%), no defects are observed in the structure. For compressions between 15% and 24%, stacking faults are produced. For compressions greater than 24%, a structural change from fcc to hcp is observed. Moreover, the density of defects in the solid is well reproduced as a function of shock strength (compression). Work is in progress to determine the effect on melting of shock propagation direction in the crystal [9].

ACKNOWLEDGMENTS

One of us (R.R.) would like to express his gratitude to CECAM and the Centre National de la Recherche Scientifique (CNRS) for financial support while on leave at CECAM in Lyon, France where part of this work was carried out. Work at Los Alamos was carried out under the auspices of the U.S. Department of Energy under Contract No. W-7405-ENG-36.

[1] See review in B. L. Holian, Shock Waves **5**, 149 (1995).
[2] B. L. Holian and P. S. Lomdahl, Science **80**, 2085 (1998); T. C. Germann, B. L. Holian, P. S. Lomdahl, and R. Ravelo, Phys. Rev. Lett. **84**, 5351 (2000).
[3] V. V. Zhakhovskii, S. V. Zybin, K. Nishihara, and S. I. Anisimov, Phys. Rev. Lett. **83**, 1175 (1999).
[4] S. Nosé, J. Chem. Phys. **81**, 511 (1984); W. G. Hoover, Phys. Rev. A **31**, 1695 (1985).
[5] M. A. Mogilevsky, in *Shock Waves and High Strain Rate Phenomena in Metals*, edited by L. E. Murr and M. A. Meyers (Plenum, New York, 1981), p. 531.
[6] B. L. Holian, A. F. Voter, and R. Ravelo, Phys. Rev. E **52**, 2338 (1995).
[7] J. B. Gibson, A. N. Goland, M. Milgram, and G. Vineyard, Phys. Rev. **120**, 1229 (1960).
[8] F. Milstein and B. Farber, Phys. Rev. Lett. **44**, 277 (1980).
[9] V. V. Zhakhovskii, S. V. Zybin, and K. Nishihara, in *Proceedings of the Symposium on Shock Waves* (Tokyo University Press, Japan, 2000), p. 262.
[10] J. Belak (private communication).